Highly stretchable 3d-printed composite structures

Sarvestani, H. Yazdani; Niknam, H.; Akbarzadeh, A. H.; Jakubinek, M. B.; Ashrafi, B.

Publisher's version / Version de l'éditeur:

Proceedings of the 2019 International Conference on Composite Materials, International Conference on Composite Materials (ICCM), 2019-08-16

TWENTY-SECOND INTERNATIONAL CONFERENCE ON COMPOSITE MATERIALS (ICCM22)

HIGHLY STRETCHABLE 3D-PRINTED COMPOSITE STRUCTURES

H. Yazdani Sarvestani [1, 3]*, H. Niknam [3], A.H. Akbarzadeh [2, 3], M.B. Jakubinek [4] and B. Ashrafi [1]
[1] Structures, Materials and Manufacturing Laboratory, National Research Council Canada (NRC), Montreal, Canada
[2] Department of Mechanical Engineering, McGill University, Montreal, Canada
[3] Bioresource Engineering Department, McGill University, Montreal, Canada
[4] Security & Disruptive Technologies Research Center, NRC, Ottawa, Canada
*Corresponding authors: (hamidreza.yazdani@nrc.ca)

Keywords: Large deformation; 3D-printed composites; Architected materials; Homogenization.

ABSTRACT

In this study, the large deformation behaviour of 3D-printed structures with representative arrowhead shape topology is studied and compared with the corresponding responses of conventional hexagonal structures. Polymer and nylon specimens were manufactured by 3D printing. Quasi-static uniaxial tensile tests were conducted followed by finite element (FE) simulations. The deformation, tensile stress-strain curves and energy absorption of these architected composites are investigated. In addition, the standard mechanics homogenization is implemented through FE modelling to accurately predict the effective mechanical properties of arrowhead shape structures. A good agreement is observed between the results of detailed FE modelling and homogenization predictions. Subsequently, the effect of initial arrowhead angle is studied using FE analysis.

1. INTRODUCTION

Additive manufacturing (AM) has gained great attention in recent years as it allows the creation of complex 3D geometries, which enable new functionalities or improved performance [1]. At the same time, advances in the defense, aerospace, automotive and energy industries have triggered a tremendous demand for high-performance materials with a combination of reduced weight, high stiffness, energy absorption and fracture toughness for extreme loading conditions [2]. Structural topologies have a significant impact on the mechanical behaviour of structures and, in that sense, efforts have been devoted to design deterministic materials for new mechanical functionalities with high performance. For example, ultra-light metallic micro-lattice materials that exhibit excellent energy dissipation and recoverability have been designed and fabricated [3]. Highly stretchable structures with high-performance have been used for different applications such as stretchable sensors [4], wearable electronics [5, 6], morphine structures [7] and health monitoring systems [8]. A core challenge in each of these systems is to realize a high level of stretchability while still achieving suitable performance in other respects (e.g., in the electronic performance failure strength or energy absorption). Although a few studies have been performed on stretchable soft materials [9], less attention has been paid to systemically explore and simulate energy absorption and stretchability of 3D-printed composite structures. Here we apply polymer AM, informed by FEM simulation and mechanics homogenization, to manufacture and evaluate the performance of such structures, based on an arrowhead geometry, in comparison to conventional hexagons.

2. MATERILAS AND METHODS

2.1. Design and Fabrication

The designed structures were manufactured by 3D printing using a fused deposition modeling (FDM)/fused filament fabrication (FFF)-type printer (Prusa i3). Samples were printed in Nylon or a short carbon fiber-reinforced Nylon (Onyx, MarkForged) composite, and PLA. The arrowhead and hexagonal shape structures as shown in Fig. 1.

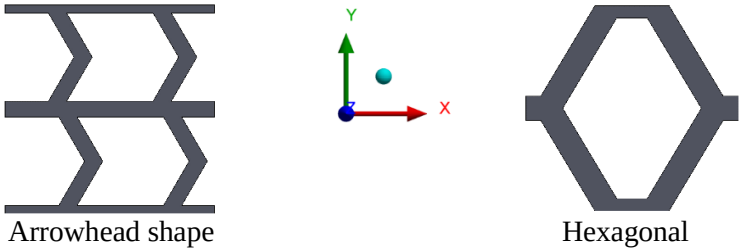

Fig. 1. Unit cells of architected composites.

2.2. Novel Sinusoidal Accordion-like Structure

As it could be observed in the last section, arrowhead structures may undergo larger strain compared to the hexagon and re-entrant honeycombs; however, their stretching capacity is limited by sharp edges in the middle. These sharp edges lead to stress concentration and failure before other portions of the structure. Therefore, in order to enhance the stretchability of the arrowhead structures these sharp edges must be avoided. Consequently, we replaced two straight links of the arrowhead structure with different sinusoidal curves as demonstrated in Fig 2.

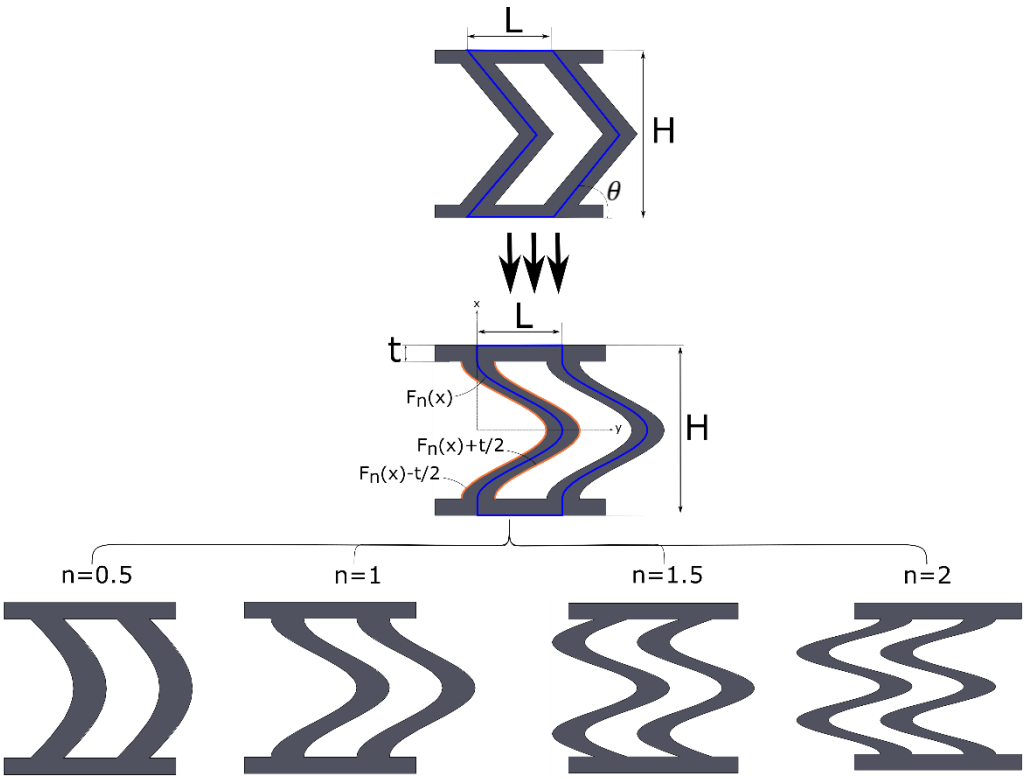

Fig. 2: Accordion-like sinusoidal structure for increasing stretchability.

The curves that form the struts of the accordion-like structures are defined by the following equation:

$$F_n(x) = \frac{L}{2}\cos\left(\frac{2\pi n}{1-\frac{H}{t}}\right), \tag{1}$$

where n determines the period of the function.

2.3. Experimental Test Configurations

Uniaxial tensile tests were conducted by using MTS machine with a load cell of 100 kN. Architected 3D-printed composite specimens were under tension condition to evaluate their stretchability. In each test, two sides of the specimen were pin-joined, allowing the edge to rotate freely, and the other two free. One edge of the sample was attached to a fixed position while the other moved with the cross-head.

Each test was stopped at the point of fracture. Figure 3 presents the uniaxial tensile tests of 3D-printed dogbone samples.

Fig. 3: Uniaxial tensile tests of 3D-printed dogbone samples.

2.4. Homogenization

The elastic effective properties of the cellular core of the architected sandwich panels were obtained here by implementing the standard mechanics homogenization [10, 11]. In contrast to analytical models, which only provide an estimated bound for elastic properties of advanced materials, effective elastic stiffness of advanced materials can be obtained with a high degree of accuracy by implementing the standard mechanics homogenization. In this method, a representative unit cell is modeled in ANSYS mechanical APDL and is discretized with 8-node 3D Solid185 elements. Elastic periodic boundary conditions are applied on the edges of the unit cell. Then, the unit cell is subjected to six independent macroscopic unit strains as:

$$\bar{\varepsilon}_{11} = [1\ 0\ 0\ 0\ 0\ 0]^T,\ \bar{\varepsilon}_{22} = [0\ 1\ 0\ 0\ 0\ 0]^T,\ \bar{\varepsilon}_{33} = [0\ 0\ 1\ 0\ 0\ 0]^T,$$
$$\bar{\varepsilon}_{12} = [0\ 0\ 0\ 1\ 0\ 0]^T,\ \bar{\varepsilon}_{13} = [0\ 0\ 0\ 0\ 1\ 0]^T, \text{ and } \bar{\varepsilon}_{23} = [0\ 0\ 0\ 0\ 0\ 1]^T. \quad (2)$$

Solving the finite element model, the equivalent microscopic strains, ε_{ij}, are obtained for each of the above macroscopic strains. Knowing the values of $\overline{\varepsilon_{ij}}$ and ε_{ij}, the local structural tensor, M^c_{mnkl}, can be obtained according to:

$$\varepsilon_{ij} = M^c_{mnkl}\,\overline{\varepsilon_{ij}}. \quad (3)$$

The effective stiffness matrix can be simply derived by taking the integral of the microscopic stress over the unit cell and dividing by its volume:

$$\bar{C}_{ijkl} = \frac{1}{V_{RVE}} \int C_{ijmn} M^c_{mnkl} dV_{RVE}, \quad (4)$$

where C_{ijmn} (i, j, k, l, m and n = 1, 2 and 3) is stiffness matrix, V_{RVE} represents the volume of the unit cell or representative volume element (RVE). Based on homogenization, effective material density (ρ_m) is simply calculated by: $\rho_m = \rho \times \rho_s$ (ρ_m is density of cellular unit cell, ρ is relative density of unit cell and ρ_s is the material density of constituent solid materials).

2.5. Finite Element Modelling

The 3D explicit nonlinear FE analysis was conducted using commercial software ANSYS Workbench, version 19 as seen in Fig. 4. 3D-printed structures under a quasi-static uniaxial tensile displacement are simulated. The constitutive stress-strain relation of the base material (PLA in the case shown below) was obtained by performing tensile tests on dogbone sample as seen in Fig. 5. To consider failure during the large deformation of architected composites, the maximum equivalent plastic strain criterion is used. In addition, geometric nonlinearity is adopted to capture the large deformation mechanism.

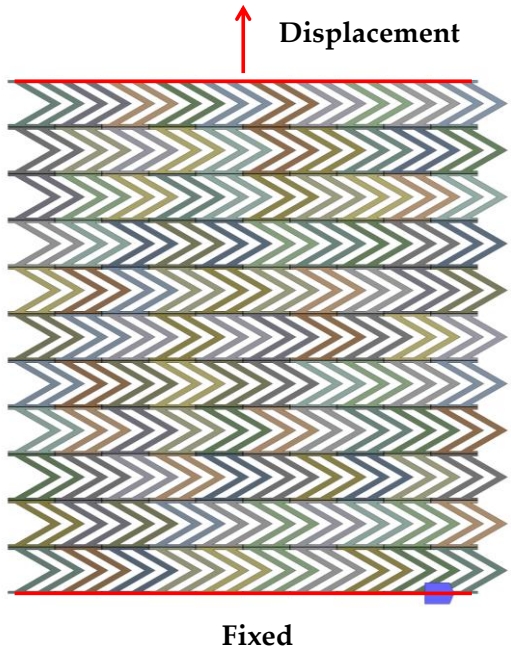

Fig. 4: FEA modeling for arrowhead structures under a quasi-static uniaxial tensile displacement.

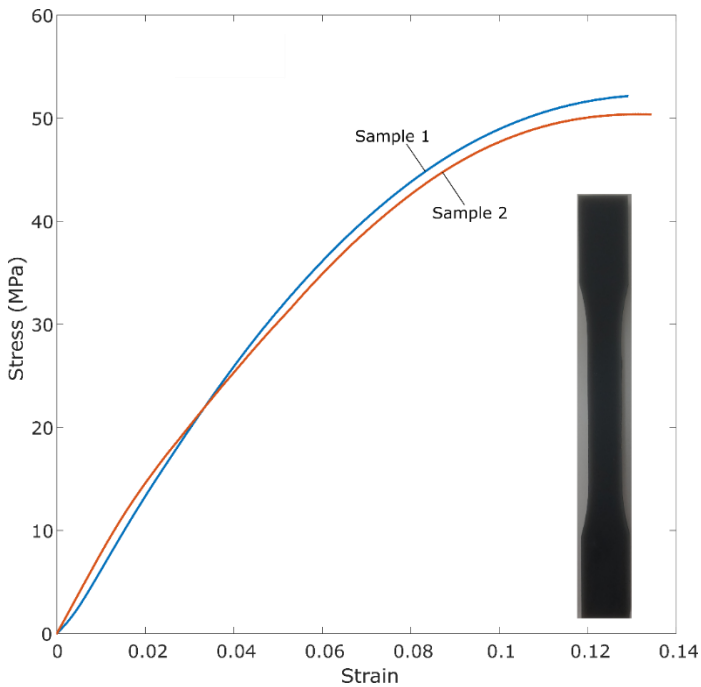

Fig. 5: Engineering stress-strain curves of 3D printed PLA coupons under tensile load.

3. RESULTS AND DISCUSSION

3.1. Stiffness

Table 1 presents the comparison between the stiffness of architected 3D-printed structures under a uniaxial displacement load in the y-direction. Good agreement is observed between the homogenization and FEA results, with less than 10% discrepancy.

Unit cell		Homogenization	FEA
Arrowhead shape	θ = 30°	0.041 GPa	0.05 GPa
	θ = 50°	0.13 GPa	0.15 GPa
	θ = 70°	0.66 GPa	0.7 GPa
	θ = 90°	0.82 GPa	1 GPa
Hexagonal shape	θ = 70°	0.58 GPa	0.73 GPa
	θ = 90°	1.08 GPa	1.2 GPa

Table 1. Stiffness based on homogenization and FEA.

3.2. Mechanical Performance

The stress-strain curves of arrowhead (θ = 30°, 50°, 70° and 90°) and hexagonal (θ = 70° and 90°) architectures are presented in Fig. 6. It is seen that the arrowhead architecture with θ = 30° can sustain much higher tensile strain and less stress level compared with other architectures. Figure 7 presents the stress-strain curves for accordion-like sinusoidal structures. It is seen that the stretchability of the structure increases with increasing *n* even though the maximum stress for failure decreases. Therefore, with increasing *n*, we can improve the stretchability of structures. However, if the amount of energy that is absorbed through the mechanical load is important, we need to optimize the structures to have not only high stretchability but also higher failure stress. This could be achieved through us of graded structures that will be investigated in later works.

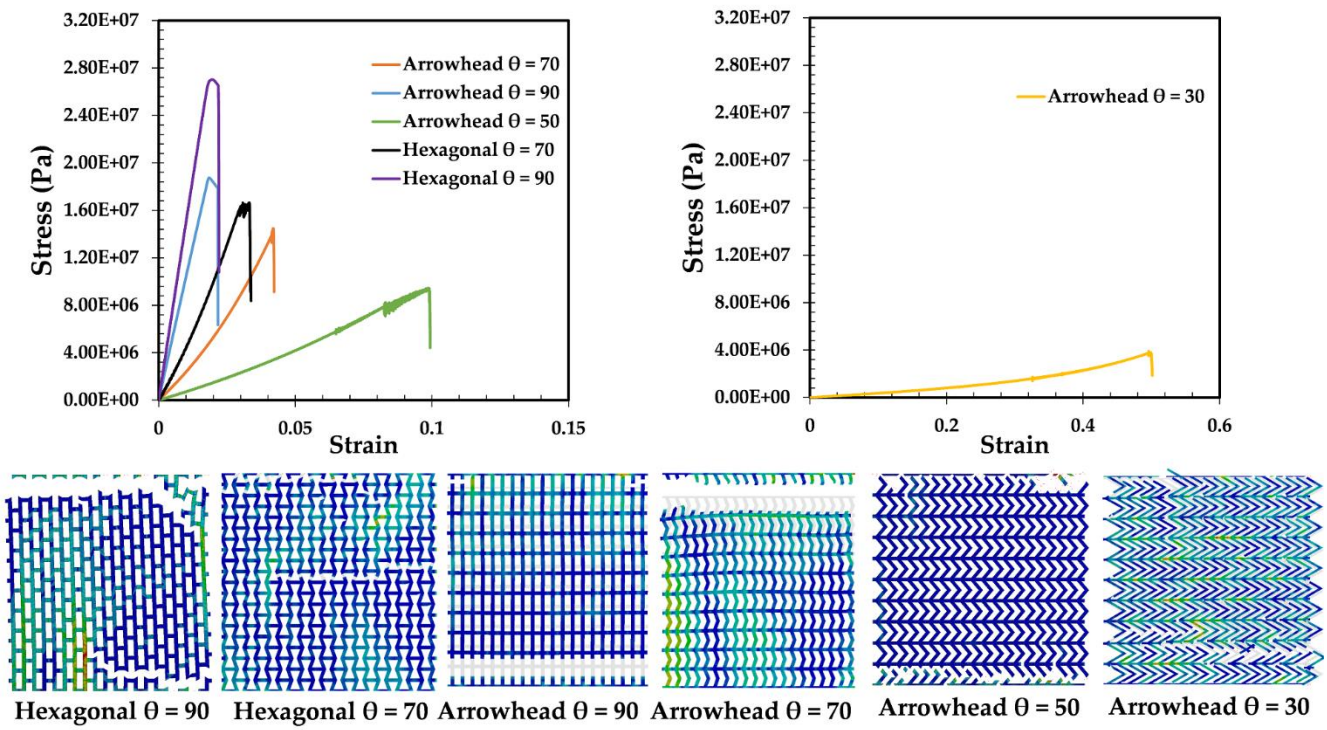

Fig. 6. FEA stress-strain curves of structuresincluding arrowhead and hexagonal shapes with a relative density of 50%.

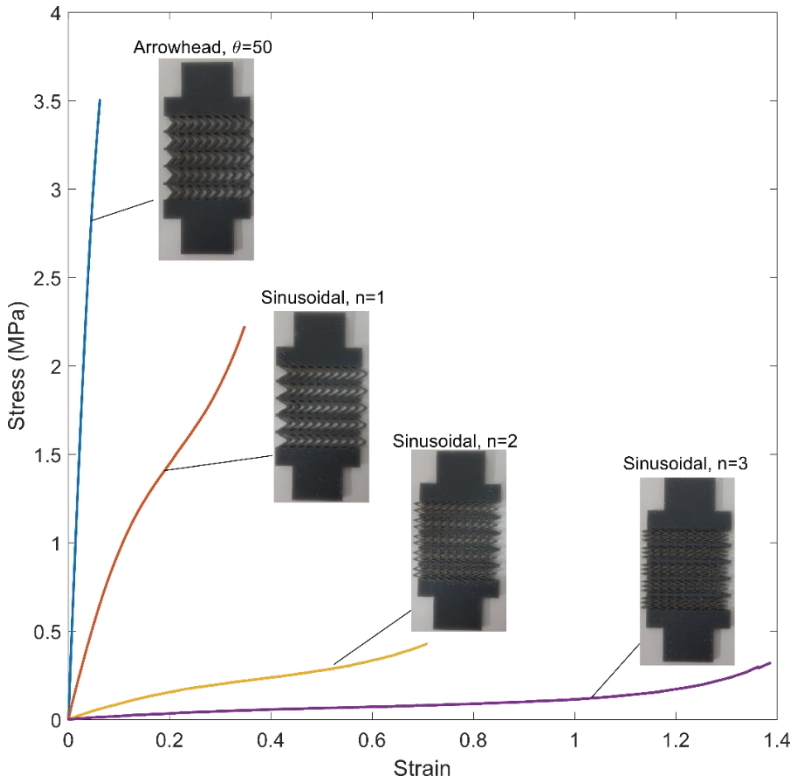

Fig. 7: Experimental stress-strain curves for accordion-like sinusoidal structures for increasing stretchability.

4. CONCLUDING REMARKS

Arrowhead, conventional hexagonal and novel sinusoidal accordion-like composite structures were investigated due to their large, tailorable deformation capability. Quasi-static tensile tests were performed on 3D-printed samples. It has been observed that the sinusoidal accordion-like structures with n = 3 can show a large strain value of 1.44. For a given density, a larger initial cell angle reduces the maximum strain in the final stage of the stress-strain curves. Finally, the design of the developed structures can be tuned according to failure strain of the energy absorption performance for the structures during the mechanical loading.

ACKNOWLEDGEMENTS

H. Yazdani Sarvestani is supported by an FRQNT (Fonds Nature et technologies) postdoctoral award. A.H. Akbarzadeh acknowledges the financial supports provided by McGill University and the Natural Science and Engineering Research Council of Canada (NSERC).

References

[1] D.K. Patel, A.H. Sakhaei, M. Layani, B. Zhang, Q. Ge, S. Magdassi, Highly stretchable and UV curable elastomers for digital light processing based 3D printing, Advanced Materials 29(15) (2017) 1606000.

[2] G. Cole, A. Sherman, Light weight materials for automotive applications, Materials characterization 35(1) (1995) 3-9.

[3] T.A. Schaedler, A.J. Jacobsen, A. Torrents, A.E. Sorensen, J. Lian, J.R. Greer, L. Valdevit, W.B. Carter, Ultralight metallic microlattices, Science 334(6058) (2011) 962-965.

[4] X. Huang, Y. Liu, H. Cheng, W.J. Shin, J.A. Fan, Z. Liu, C.J. Lu, G.W. Kong, K. Chen, D. Patnaik, Materials and designs for wireless epidermal sensors of hydration and strain, Advanced Functional Materials 24(25) (2014) 3846-3854.

[5] A.M. Hussain, F.A. Ghaffar, S.I. Park, J.A. Rogers, A. Shamim, M.M. Hussain, Metal/polymer based stretchable antenna for constant frequency far-field communication in wearable electronics, Advanced Functional Materials 25(42) (2015) 6565-6575.
[6] M.U. Rehman, J.P. Rojas, Optimization of compound serpentine–spiral structure for ultra-stretchable electronics, Extreme Mechanics Letters 15 (2017) 44-50.
[7] M. Jakubinek, S. Roy, M. Palardy-Sim, B. Ashrafi, F. Shadmehri, G. Renaud, M. Barnes, Y. Martinez-Rubi, M. Rahmat, B. Simard, Stretchable structure for a benchtop-scale morphed leading edge demonstration, AIAA Scitech 2019 Forum, 2019, p. 1857.
[8] M.S. White, M. Kaltenbrunner, E.D. Głowacki, K. Gutnichenko, G. Kettlgruber, I. Graz, S. Aazou, C. Ulbricht, D.A. Egbe, M.C. Miron, Ultrathin, highly flexible and stretchable PLEDs, Nature Photonics 7(10) (2013) 811.
[9] Y. Jiang, Q. Wang, Highly-stretchable 3D-architected mechanical metamaterials, Scientific reports 6 (2016) 34147.
[10] B. Hassani, E. Hinton, A review of homogenization and topology opimization II—analytical and numerical solution of homogenization equations, Computers & structures 69(6) (1998) 719-738.
[11] A. Akbarzadeh, J. Fu, L. Liu, Z. Chen, D. Pasini, Electrically conducting sandwich cylinder with a planar lattice core under prescribed eigenstrain and magnetic field, Composite Structures 153 (2016) 632-644.